Journal of Solid Mechanics Vol. 12, No. 2 (2020) pp. 476-492
DOI: 10.22034/jsm.2019.1876608.1482

Stiffeners Mechanical Effect Analysis by Numerical Coupling

R. Naceur Bouharkat [1], A. Sahli [1,*], S. Sahli [2]

[1]*Laboratoire de Recherche des Technologies Industrielles, Université Ibn Khaldoun de Tiaret , Département de Génie Mécanique, Route de zaroura , Algérie*
[2]*Université d'Oran 2 Mohamed Ben Ahmed, Algérie*

Received 24 March 2020; accepted 20 May 2020

ABSTRACT

Given any structure, we seek to find the solution of mechanical problem as precisely and efficiently as possible. Within this condition, the BEM is robust and promising development, standing out in the analysis of cases with occurrence of large stress gradients, as in problems of fracture mechanics. Moreover, in BEM the modeling of infinite means is performed naturally, without the use of approximations. For methods involving domain integration, such as FEM, this is not possible, as models with high number of elements are usually adopted and their ends are considered flexible supports. This paper deals with the development of numerical models based on the BEM for mechanical analysis of stiffened domains. In the modeling of hardeners, immersed in a medium defined by the BEM, we tried to use both the FEM, already present in the literature, and the BEM 1D, being a new formulation. The objective was to perform the coupling of BEM with FEM and BEM 1D for elements of any degree of approximation, evaluating both isotropic and anisotropic medium. In addition, a complementary objective was to verify the effects of the adoption of different discretization and approximation degrees on the stiffeners. However, the coupling with the BEM 1D leaded to more stable results and better approximations. It was observed that the FEM results were instable for many results, mainly in the quadratic approximations. When the approximation degree rises, the methods tend to converge to equivalent results, becoming very close in fourth degree approximation. Lastly, it was observed stress concentration in the stiffeners ends. In these regions, the discretization and the approximation degree have large influence to the numerical response.

Keywords: BEM; BEM/FEM coupling; BEM/BEM 1D coupling; Reinforced media; Stiffeners modelling.

1 INTRODUCTION

THE importance of a good representation of fiber reinforced media for engineering analysis can be identified when observing the great amount of effort in studying the phenomenological behavior of this kind of material

*Corresponding author.
E-mail address: ahmed.sahli@univ-tiaret.dz (A. Sahli).

and various alternatives present in commercial software or scientific papers in order to solve this kind of problem (Barzegar; Maddipudi, [1]; Gomes; Awruch, [2]). Highlighting the importance of mechanical analysis of stiffened domains, several works in the literature seek alternatives to find their solution and better representation. The governing equations of the problem to be solved are presented as differential equations, solved analytically or numerically. However, the analysis of the joint behavior of materials of different mechanical properties can present great complexity. In the case of stiffened domains, for example, structural elements are used that are shaped differently, such as lattice boards or beamed shells. Analytical solutions are limited to restricted cases, requiring several simplifications, and for this reason are of restricted use. By involving approximations only in the boundary of the problems, BEM offers adequate solutions for fracture mechanics. In Le Van; Royer, [3], the case of anisotropic three-dimensional fracture for the finite and infinite case is studied. Already in Leonel, [4], BEM is used in the analysis of multi-fractured bodies, later (Leonel, [5]) presents models representing the process of growth of cracks in flat domains consisting of fragile, quasi-fragile and ductile materials. In fracture models, the dual BEM formulation is used. The work also presents the expressions of tangent operators, used in nonlinear formulations in linear and cohesive elastic fracture problems, contact problems and stiffened domain problems. In Oliveira; Leonel, [6-7], the propagation of fracture in quasi-fragile materials is studied through an alternative formulation of BEM, where an initial stress field is used to represent the cohesive zone. In order to accelerate the convergence of the solution, the tangent operator is used. Results are compared with experimental data and dual BEM. It is also important mentioning some works dealing with failure and cracked anisotropic bodies in the context of BEM (Nourine et *al*., [8]; Sahli et *al*., [9]; Sahli et *al*., [10]*;* Debbaghi et *al*., [11]; Kebdani et *al*., [12]; Sahli et *al*., [13]; Kadri et *al*., [14]; Sahli and Sara, [15]).Typically, BEM / FEM coupling is performed for adjacent sub regions, where their interface is coupled. In the case of reinforced domains, the stiffener, despite being differently modeled, lies within the sub region modeled by BEM. This section will present texts that refer to the coupling between adjacent sub regions. The BEM / FEM coupling in structural engineering was initially proposed by (Zienkiewicz; Kelly; Bettess, [16]) and (Falby; Shawt, [17]). In the work of Brebbia; Georgiou, [18], two-dimensional problems were evaluated through this coupling. The usefulness of the coupling is evidenced in the work of (Wearing; Burstow, [19]) being used for the analysis of elastoplastic and mechanical problems of conventional elastoplastic fracture. In (Coda; Venturini; Aliabadi, [20]) and (Coda; Venturini, [21]), the coupling for the static and dynamic three-dimensional elastic case is studied. In (Elleithy; Tanaka; Guzik, [22]), is made the BEM / FEM coupling, considering elastoplastic analysis. In Ganguly; Layton; Balakrishna, [23], the BEM / FEM coupling is performed symmetrically, making the resolution of linear systems faster. In Bia et al., [24], the coupling is carried out between (BEM / FEM, BEM / BEM) and (BEM and FEM) / analytical solutions. In the case of stiffened domains, as stated above, the stiffener lies within the sub-region modeled by BEM, with efforts to be determined. The use of reinforced materials has numerous applications in industry, in the case of the aeronautical industry for example, the numerical analysis of their use is performed using both the formulation of BEM and FEM. On the other hand, only the formulation of BEM is used. In Coda, [25], the BEM / FEM coupling for reinforced media is developed aiming at both static and dynamic analysis. The formulation of FEM is performed in such a way that their nonlinear influences are considered as residual forces in the BEM matrix. (Leite; Coda; Venturini, [26]) and (Fernandes; venturini, [27]) applied the BEM-FEM coupling for plate problems, analyzing cases of reinforced concrete slabs.

In this paper, the author wishes pointing out some relevant works. Coupling techniques, in which BEM equations are combined with algebraic relations coming from other numerical methods, are possible choices that engineers can follow to solve practical problems.

2 COUPLING BEM – STIFFENING

Consider a two-dimensional domain Ω, wherein Γ represents the regular boundary (Fig. 1). The displacement boundary integral equation relating the boundary displacements u_k with the boundary tractions p_k in the presence of body forces b_k can be written as:

$$cu_k + \int_\Gamma p_{ik}^* u_k \, d\Gamma = \int_\Gamma p_k u_{ik}^* \, d\Gamma + \int_\Omega b_k u_{ik}^* \, d\Omega \tag{1}$$

where i, k denote Cartesian components, and p_{ik}^* and u_{ik}^* represent the traction and displacement fundamental solutions at a boundary point due to a unit load. The term c is generally a function of the geometry variation at the boundary point, it can be shown that $c_{ik} = ½\ \delta_{ik}$ (Brebbia and Dominguez, [28]).

Differentiation will be performed between the BEM / FEM coupling for adjacent subregions and the BEM coupling with stiffeners. In case of BEM / FEM coupling to adjacent subregions, only the interface between the methods will be coupled. Displacements compatibility is imposed, i.e. for the boundary of the two subregions the displacement will be the same. Moreover, equilibrium is imposed, which in this case means that the surface forces for the two subregions are of the same absolute value and opposite, that is, they cancel each other out. Otherwise, in the BEM coupling with hardeners, they are present in any direction within the BEM domain, which will be called the Domain. In the formulation of BEM, the medium is considered homogeneous. In order to take into account, the existence of stiffeners, effects overlapping is then used, and the coupling is performed by applying the conditions of compatibility and equilibrium on the fiber nodes.

Stiffeners, also called fibers, have been adopted that are linear with rigidity only in the axial direction, i.e. truss elements. As performed by (Leonel, [5]) for the BEM / FEM coupling, the two methods are used separately for overlapping effects.

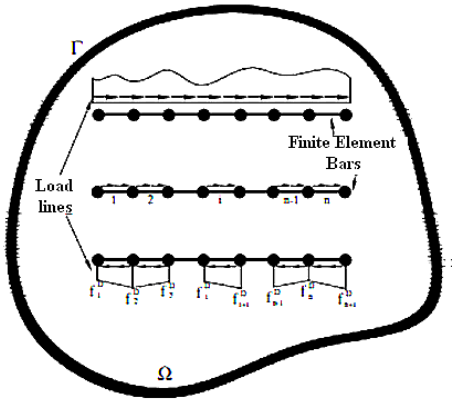

Fig.1
BEM / FEM coupling. (Leonel, [5])

The adhesion between stiffeners and the Domain causes the emergence of distributed forces, these are called load lines or adhesion forces. By equilibrium, the applied force on the fiber must be opposite to the applied load on the Domain, that is:

$$f^D = -f^F$$

where f^D and f^F are forces on the Domain and on the fiber respectively.

Disregarding the slip of the fibers, the displacement in their points should be the same for both methods, i.e.:

$$u^D = u^F$$

Using the BEM formulation for the boundary from the Somiglian Identity, Eq. (1), the following equation is obtained:

$$H_{CC} u_C = G_{CC} p_C + G_{CF} f^D \tag{2}$$

where the first index indicates the location of the source point and the second the location of the elements integrated by it, i.e.:

H_{CC} is the matrix H obtained by BEM for the boundary points integrated in the boundary.

G_{CC} is the matrix G obtained by BEM for the boundary points integrated in the boundary.

G_{CF} is the matrix G obtained by BEM for the boundary points integrated in the fiber.

Using the BEM formulation for the hardener gives the following equation:

$$u_F + H_{FC} u_C = G_{FC} p_C + G_{FF} f^D \tag{3}$$

H_{FC} is the matrix H obtained by BEM for the fiber points integrated in the boundary.

G_{FC} is the matrix G obtained by BEM for the fiber points integrated in the boundary.

G_{FF} is the matrix G obtained by BEM for fiber points integrated into the fiber.

To conclude the coupling is missing the algebraic equation of the stiffener itself, it can be written as follows:

$$K_F u_F = G_F f^F \tag{4}$$

where K is the stiffness matrix.

The difference between the methods used to model the hardener only occurs in obtaining this last equation, regardless of whether the medium is isotropic or anisotropic. For the case of the BEM / FEM coupling, approximation is required for both displacements and distributed force. Using the BEM / BEM 1D coupling, requires approximation of the distributed force only. Joining Eqs. (2), (3) and (4) gives:

$$\begin{bmatrix} H_{CC} & 0 & -G_{CF} \\ H_{FC} & I & -G_{FF} \\ 0 & K_F & G_F \end{bmatrix} \begin{Bmatrix} u_C \\ u_F \\ f^D \end{Bmatrix} = \begin{Bmatrix} G_{CC} \\ G_{FC} \\ 0 \end{Bmatrix} p_C \tag{5}$$

This way one can finally get the problem solved by performing the column exchange process. It is observed that the load lines are unknowns of the problem, to obtain them, it is necessary to use approximate functions. The Finite Element technique is adopted to perform its approximation, so that its nodal values are obtained. In the case of coupling with the MEF, the same degree of approximation is adopted, so for all nodes of the problem displacement and the force of adhesion results are obtained. In addition, the MEF formulation was adopted where elements of any degree of approximation can be used, and then the matrices were constructed by numerical integration.

3 ONE-DIMENSIONAL BOUNDARY ELEMENT METHOD (BEM 1D)

(Cruz, [29]) presents the fundamental solution for the BEM 1D. Through this solution, it is possible to develop the formulation for the case of truss bars with distributed forces, necessary for the representation of the stiffener in a boundary element mesh.

The equilibrium of a truss bar is given by the following equation:

$$\frac{dN(x)}{dx} = -p(x) \tag{6}$$

where $N(x)$ is the normal force on the element, $p(x)$ is the distributed force on the element and x is the longitudinal axis.

Applying the constitutive relationship and the compatibility relationship, we obtain the relationship:

$$N(x) = EA \frac{du(x)}{dx} \tag{7}$$

where E is the longitudinal modulus of elasticity, or Young's modulus, A is the cross-sectional area.

Substituting Eq. (6) into Eq. (7) gives the governing equation of the lattice bar problem in terms of displacement:

$$EA \frac{d^2u(x)}{dx^2} = -p(x) \tag{8}$$

Let u^* be the weight function, the direct variational form is given by:

$$\int_0^L \left(EA \frac{d^2u(x)}{dx^2} + p(x) \right) u^* dx = 0 \tag{9}$$

Integrating by parts:

$$\left[EA\frac{du(x)}{dx}u^*\right]_0^L-\int_0^L\left[\frac{du}{dx}EA\frac{du^*}{dx}-p(x)\right]u^*dx=0 \tag{10}$$

Integrating the second term by parts again:

$$\left[EA\frac{du(x)}{dx}u^*\right]_0^L+\int_0^L\left[u(x)EA\frac{d^2u^*}{dx^2}+p(x)\right]dx=0 \tag{11}$$

The weight function u^* is chosen so that relations (7) and (8) are valid. Substituting these relationships in Eq. (11) gives:

$$\left[N(x)u^*\right]_0^L-\left[u(x)N^*\right]_0^L=\int_0^L u(x)p^*dx-\int_0^L p(x)u^*dx \tag{12}$$

The BEM 1D differential is the choice of the weight function p^*. As for the BEM, we chose to avoid domain integration, using for this the Dirac Delta, as follows:

$$p(x,\hat{x})=\Delta(x,\hat{x}) \tag{13}$$

$\Delta(x,\hat{x})$ is the Dirac Delta;
x is the point to be evaluated, called Field Point;
$\hat{x}$ is the application point of the Dirac Delta, called the Source Point.
The solution of the previous equation is called the BEM 1D Fundamental Solution.
This way, the integration of displacement in the domain is no longer necessary:

$$\int_0^L u(x)p^*(x,\hat{x})dx=u(\hat{x}) \tag{14}$$

Eq. (12) then takes the following form:

$$u(\hat{x})+\left[u(x)N^*(x,\hat{x})\right]_0^L=\left[N(x)u^*(x,\hat{x})\right]_0^L+\int_0^L p(x)u^*(x,\hat{x})dx \tag{15}$$

Through this equation and using the fundamental solution we find the answer to the lattice element boundary, i.e. its ends. The Fundamental Solution is found in (Cruz, [29]) :

$$u^*(x,\hat{x})=-\frac{|x-\hat{x}|}{2EA} \tag{16}$$

$$N^*(x,\hat{x})=EA\frac{du^*(x,\hat{x})}{dx}=-\frac{1}{2}\mathrm{sgn}(x-\hat{x}) \tag{17}$$

The following nomenclature will be adopted:

$N_{ij}^*(x,\hat{x})$ $\quad i\rightarrow$ Source Point $\quad j\rightarrow$ Evaluated Point

For a bar with n nodes, the extreme nodes are evaluated:

$$\begin{Bmatrix} u_1 \\ u_n \end{Bmatrix}_L + \begin{bmatrix} -N_{11}^* & N_{1n}^* \\ -N_{n1}^* & N_{nn}^* \end{bmatrix} \begin{Bmatrix} u_1 \\ u_n \end{Bmatrix}_L = \begin{bmatrix} -u_{11}^* & u_{1n}^* \\ -u_{n1}^* & u_{nn}^* \end{bmatrix} \begin{Bmatrix} N_1 \\ N_n \end{Bmatrix} + \begin{Bmatrix} q_1 \\ q_n \end{Bmatrix} \tag{18}$$

The first line refers to source point 1 and the second to source point n. In addition, the following distributed force integrals vector was defined:

$$q_i = \int_0^L p(x) u^*(x, \hat{x}_i) dx \tag{19}$$

But the normal forces in the equation are not in the local axes, the positive value is indicating tensile force and negative compression. To leave them on the local axis we have:

$$\begin{Bmatrix} N_1 \\ N_n \end{Bmatrix} = \begin{Bmatrix} -N_1 \\ N_n \end{Bmatrix}_L \tag{20}$$

That is:

$$\begin{bmatrix} 1-N_{11}^* & N_{1n}^* \\ -N_{n1}^* & 1+N_{nn}^* \end{bmatrix} \begin{Bmatrix} u_1 \\ u_n \end{Bmatrix} = \begin{bmatrix} u_{11}^* & u_{1n}^* \\ u_{n1}^* & u_{nn}^* \end{bmatrix} \begin{Bmatrix} N_1 \\ N_n \end{Bmatrix}_L + \begin{Bmatrix} q_1 \\ q_n \end{Bmatrix} \tag{21}$$

Otherwise, naming matrices:

$$[A]\{u\}_L = [B]\{N\}_L + \{q\} \tag{22}$$

The above equation can also be written as:

$$[B]^{-1}[A]\{u\}_L = \{N\}_L + [B]^{-1}\{q\} \tag{23}$$

The aim is to calculate the distributed force integrals qi. Making change of space gives:

$$q_i = \int_{-1}^{+1} p(\xi) u^*(\xi, \xi_i) J d\xi \tag{24}$$

where J is the Jacobian of the function.

It is observed that so far, no approximations have been introduced. However, in the BEM / BEM 1D coupling, it is necessary to approximate the distributed forces on the stiffener, which are the forces transmitted to it by the medium in which, Domain is inserted. To perform the approximation, one must use the finite element technique through the form functions, with b_i being the nodal values of the distributed force:

$$p(\xi) = \phi(\xi) b_i \tag{25}$$

Since distributed forces are defined by nodal values, the concept of linear, quadratic elements, etc., is maintained. However, this will only mean that distributed forces are approximated by this degree of approximation within the element.

Introducing Eq. (25) into Eq. (24) gives:

$$q_i = \int_{-1}^{+1} \phi_j(\xi) u^*(\xi, \xi_i) J d\xi b_j \tag{26}$$

One can then write:

$$\{q\} = [C]\{b\}_L \tag{27}$$

where [*C*] is given by:

$$C_{ij} = \int_{-1}^{+1} u^*(\xi, \xi_i)\phi_j(\xi) J d\xi \tag{28}$$

Replacing Eq. (27) in (23):

$$[B]^{-1}[A]\{u\}_L = \{N\}_L + [B]^{-1}[C]\{b\}_L$$

This equation format is similar to that used in the FEM; however, it is only valid for the boundary of the elements. For the format to become the same, it is necessary to include in the previous equation the internal points of the elements.

4 BEM 1D - VALIDATION AND APPLICATION

In order to validate the implemented formulation, structures whose mechanical responses are known will be analyzed. First, the BEM 1D formulation with elements in the same direction will be tested and then tested with rotating element.

4.1 MEC 1D - Example 1: Quadratic distributed force element

We will now evaluate the case of a quadratic-governed distributed force element of the following equation:

$$p(x) = a.x^2$$

Then we have:

$$u''(x) = -\frac{ax^2}{EA}$$

Integrating and applying the essential boundary condition gives the analytical solution:

$$u(x) = -\frac{a.x^4}{12EA} + \frac{a.L^3.x}{3EA}$$

The support reaction *R* is then given by:

$$R = -N(0) = -\frac{aL^3}{3}$$

Results of the MEC 1D formulation with 5 nodes were again compared, using 4 linear elements, 2 quadratic elements or 1 element of the fourth degree. It was adopted:

$$a = 1; \qquad L = 6.$$

The error of the results was calculated, using the following formula:

$$Error = \left| \frac{x_{BEM\ 1D} - x_{FTOOL}}{x_{FTOOL}} \right|$$

where x is the variable being evaluated, F tool is a computer program.

The result can be seen in the following figure:

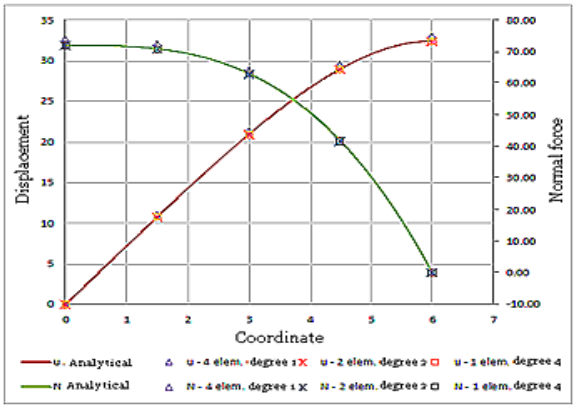

Fig.2
MEC 1D Response - Quadratic distributed force.

In the case of quadratic and fourth degree elements, the maximum error was 2.39E-15, which can be considered to coincide with the analytical response. However, in the case of using linear elements, a relevant error was obtained, 3,13E-02. The error is justified by the fact that the distributed force is described by the Finite Element Technique, according to Eq. (25). That is, as it is defined through nodal values, with the use of linear elements, it is also being considered linear within the elements. As quadratic distributed force was adopted, when considering it linear within the elements, an error occurs. Increasing bar discretization is an option to reduce this error.

The last configuration was re-analyzed using 41-node elements. Using MEC 1D, the number of nodes has less influence on the result, since in practice the solution is through the contour nodes. The response to internal nodes is obtained by post processing.

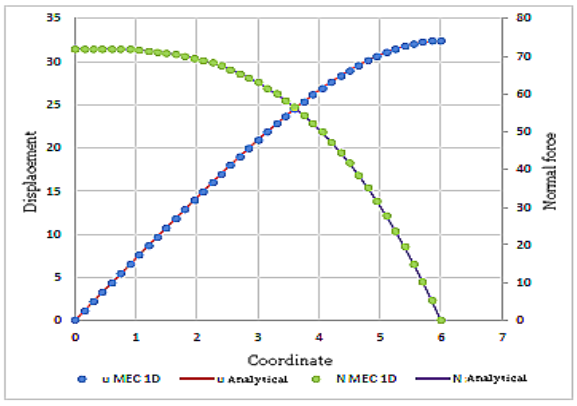

Fig.3
MEC 1D Response, 41 Nodes - Quadratic distributed force.

Good results were obtained using the method in several cases with different loading conditions. It was clear that for the influence of the approximation degree adopted for distributed force; the use of approximation degree lower than the applied force leads to an increase in the error. In this case, increasing the discretization of the element would reduce this error.

4.2 Coupling - Example 2

First, it was simulated in the ANSYS and through the BEM in coupling with the FEM and BEM 1D, an EPT panel with 3 stiffeners is used. As a support condition, the left side was set, distributed forces were applied in both the upper boundary and the right boundary, generating bending and pulling forces, respectively.

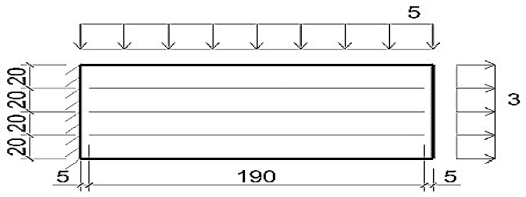

Fig.4
Panel model with stiffeners.

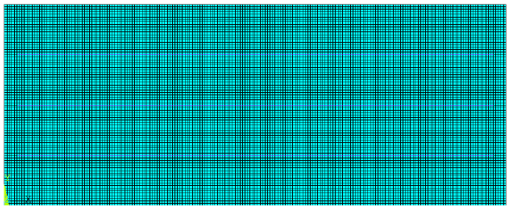

Fig.5
ANSYS model - Example 2.
(Measured in *cm*, loads in *kN / m*) - Example 2.

The concrete was considered as a linear isotropic medium. The following mechanical properties were adopted for the domain (subscript *C*) and the stiffeners (subscript *S*):

$E_S = 200\ GPa;\ E_C = 25\ GPa;\ v_C = 0.25;\ A_S = 10\ cm^2$ *(per stiffener)*

Through ANSYS, the medium was modeled using squares of quadratic approximation, of the type "PLANE 42". Tighteners were modeled using linear approach truss elements, of the "LINK 1" type. In total, 16000 elements were adopted in the middle and 190 elements for each rigger, defined based on previous study of mesh convergence, resulting in a good response behavior. The mesh used for ANSYS analysis is shown in Fig.5. In the case of the coupling analysis of the BEM with stiffeners, the medium was modeled using the BEM, using 16 boundary elements of quadratic approximation. For the analysis of displacements and support reactions, the boundary was linearized counterclockwise from the lower left vertex, the position being identified as *S* in the graphs. It is important to note that the consideration of positive or negative values for traction or compression is not used, results will be positive when its direction coincides with the direction of the axis. As for stiffeners, modeled by FEM and BEM 1D first, a comparative analysis will be performed in relation to its discretization, evaluating results for 23, 51 and 111 nodes with quadratic approximation elements, with 11, 25 and 55 elements respectively, results are presented in item 5.1.1. Then, the effect of changing the degree of approximation of the elements of the riggers will be evaluated, and the results will be presented in item 5.1.2. To evaluate results, effects of panel flexion and traction were discussed separately. Results of displacements, normal forces and grip strength were presented. In order to aid in interpretation, the graph of the latter was presented to the right side of the normal force graph. In addition, within each item we tried to use the same axis limits, allowing a more direct comparison between graphs.

Since strength concentration was expected at the tip of the stiffeners, smaller elements were used in these areas. By varying the discretization and degree of approximation, it was observed that the creation of irregular elements in these areas led to a greater increase of the error, this situation was avoided.

4.2.1 Changing discretization

First, different fiber discretizations were evaluated, verifying the mechanical effects on the boundary of the problem and on the stiffeners themselves.

4.2.1.1 Outline results

In the case of the boundary, the discretization variation of stiffeners did not influence the result. It is observed that the lower side of the panel has negative displacement at *x* and the upper side positive displacement, larger in modulus, the results obtained are expected since it is a panel subjected to flexion-traction:

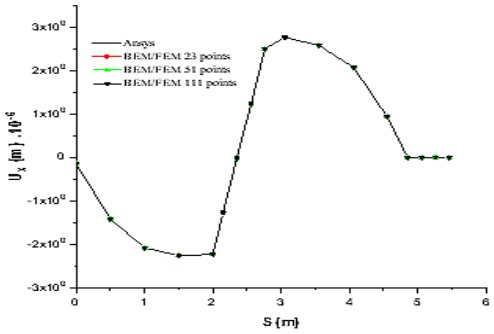

Fig.6
Displacements in the direction *x* – Coupling Example. 2, discretization.

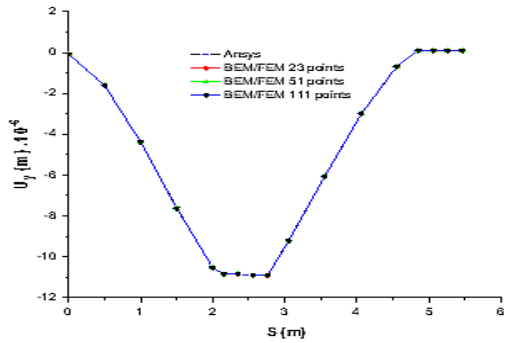

Fig.7
Displacements in the direction *y* - Coupling Example. 2, discretization.

In both directions the displacements were of small value, thus guaranteeing the validity of the regime of small displacements and deformations. In the case of displacements in *y*, the whole boundary had a negative result. Expected result due to the effects of applied flexion.

As for the supportive reactions, it was observed a greater concentration in the extremities, with increasing values. The crimping is located on the left side of the panel, initially negative values indicate that the reactions are in the opposite direction to the *x* axis, thus being traction. Positive values indicate compression. Traction values exceed the compression, being compatible with a panel subjected to flexo-traction. It is observed that through ANSYS higher stress concentrations are obtained near the ends of the boundary where the displacement is zero. This is expected due to the domain discretization required by the FEM.

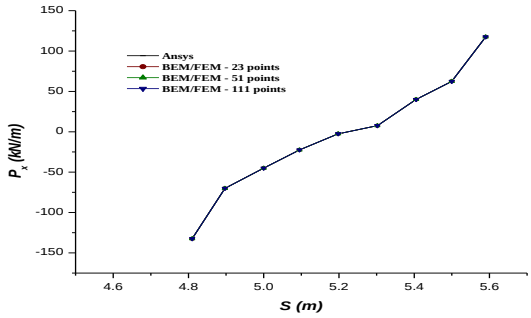

Fig.8
Support reactions in the *x* direction – Coupling Example. 2, discretization.

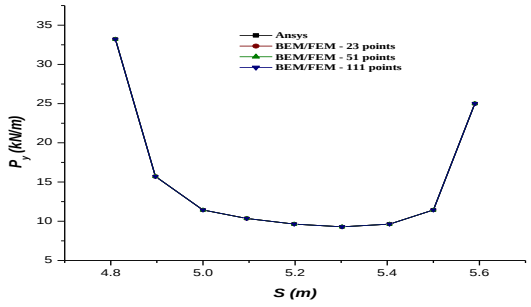

Fig.9
Support reactions in the *y* direction - Coupling Example. 2, discretization.

The support reactions in the *y* direction are due to the shear stress generated in the panel, it is observed that there is tension concentration in the ends of the crimping.

4.2.1.2 Lower fiber

In the case of the inferior fiber, the results in displacements were also close. The discretization of stiffeners had little or no influence on these results.

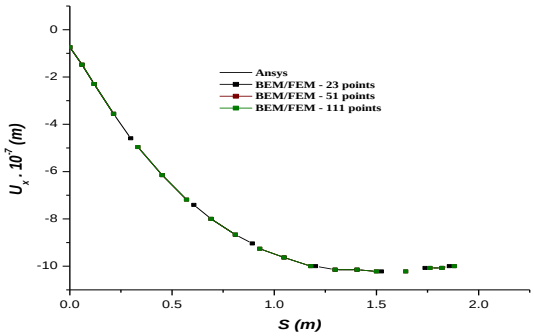

Fig.10
Displacements in *x*, in the lower fiber - Coupling Example. 2, discretization.

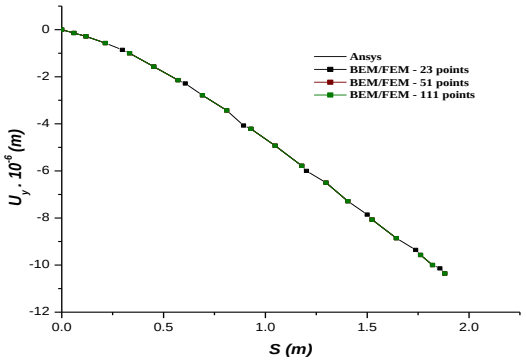

Fig.11
Displacements in *y*, in the inferior fiber - Coupling Example. 2, discretization.

Negative displacements were obtained in *x* and *y* and normal negative forces, indicating compression, that is, the effects of panel flexion exceeded traction in this fiber.

In the case of normal forces and adhesion forces, a significant perturbation in the results of the BEM / FEM coupling is observed in comparison with the BEM / BEM 1D for less discretized fibers, with 23 nodes. There is also a clear concentration of stresses at the left end of the fiber.

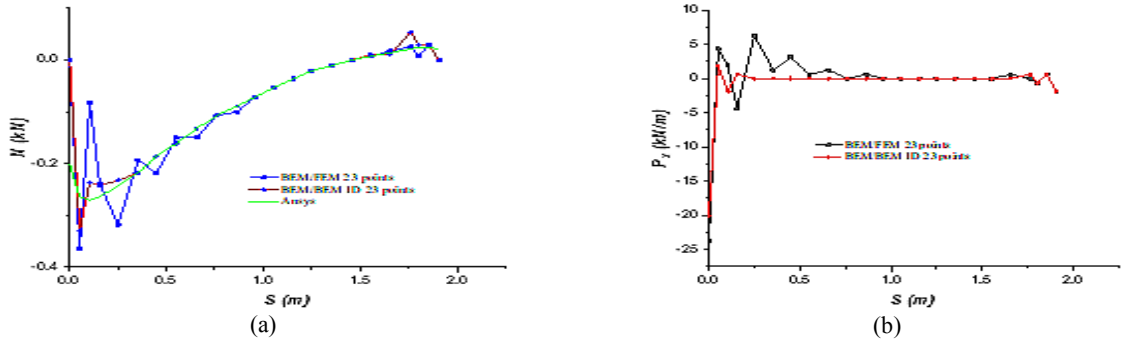

(a) (b)

Fig.12
Normal forces on the lower fiber - 23 knots – Coupling Example. 2, discretization.

with increasing discretization, the results are approaching but with some disturbance of the BEM / FEM coupling. The result of grip strength at the fiber tip increases with increasing discretization, as shown in the following figures.

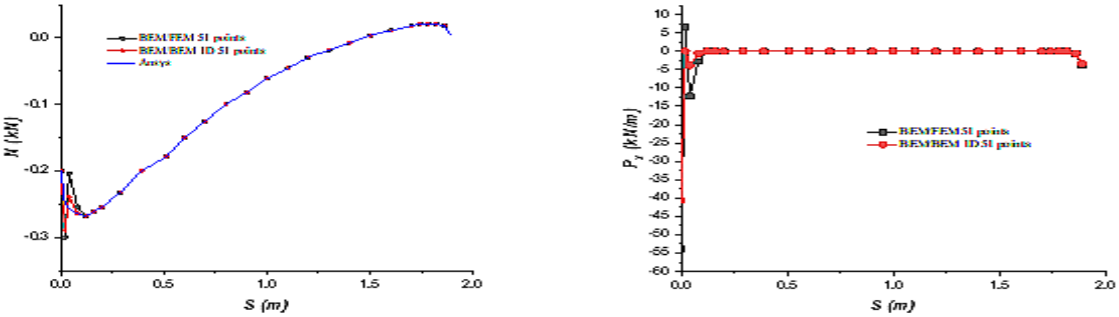

(a) (b)

Fig.13
Normal forces on the lower fiber - 51 knots - Coupling Example. 1, discretization.

The example was first studied with quadratic approximation elements and several stiffening discretizations, 23, 51 and 111 knots. In all cases good results were obtained for the boundary and the displacements of the fibers. With the increase in discretization, the usual improvement of results was obtained and it was clearly possible to notice that there is stress concentration at the fiber ends. The BEM / BEM 1D coupling had superior results in all analyzes performed, especially in the case of 23 knot discretization, with significant disturbance of the result in bond strengths and normal force in the coupling with the FEM.

Based on the previous result, the example was reassessed by varying the degree of approximation, keeping the number of fiber nodes at 23. It was found that increasing the degree of approximation has a positive effect, especially for normal force results. The BEM / BEM 1D coupling again had superior results, however in the case of approximation of the fourth degree the BEM / FEM results became close.

4.3 Coupling - Example 3

In order to validate the hardening coupling of BEM for the anisotropic case, a model with the same anisotropic material as in the previous example was proposed, but with isotropic material inclusions and more adverse loading and binding conditions.

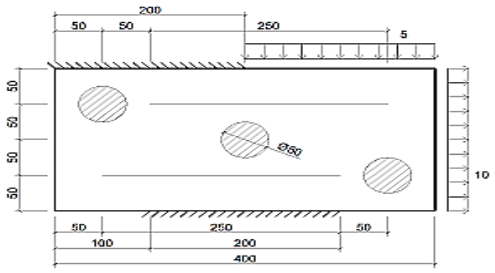

Fig.14
Anisotropic model with inclusions (hatched) and adverse conditions (measured in *cm*, loadings in *kN / m*) - Example 3.

Stiffeners Properties: $E_s = 210\ GPa$; $A_s = 10\ cm^2$ (per stiffener)

Inclusions Properties: E_c=25 GPa; νC=0,25

The medium was modeled using the BEM using 24 quadratic boundary elements. For analysis of displacements and support reactions the boundary was linearized counterclockwise starting from the lower left point.

The inclusions were modeled using 12 quadratic boundary elements each, totaling 36 boundary elements. Stiffeners were modeled with 51 knots, with quadratic and fourth degree elements, as follows:

- Degree 2: 25 elements of degree 2
- Degree 4: 12 elements of degree 4, 1 element of degree 2

As for the ANSYS model, a previous mesh convergence study was performed, which was not shown here for simplicity, reaching the following configuration:

- 100 elements in stiffeners - lattice elements (“Link1”)
- 2225 elements in isotropic inclusions - quadratic plate elements (“Plane183”)
- 4316 anisotropic elements - linear plate elements (“Plane182”)
- Detail of isotropic inclusion.

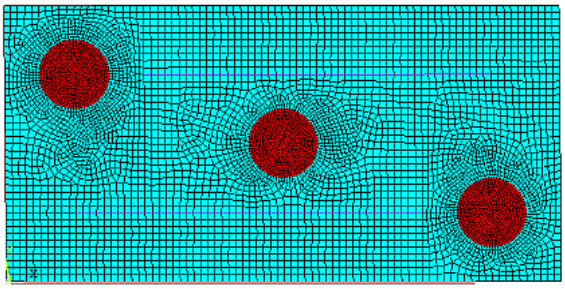

Fig.15
ANSYS model – Example. 3.

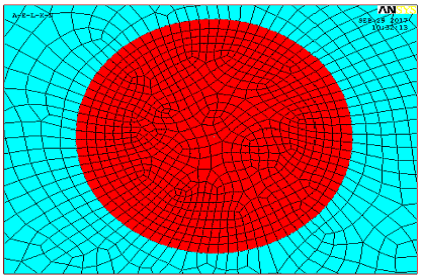

Fig.16
Detail of isotropic inclusion in ANSYS.

4.3.1 Results on the boundary

Again, close results were obtained for contour displacements, regardless of the method used to discretize it:

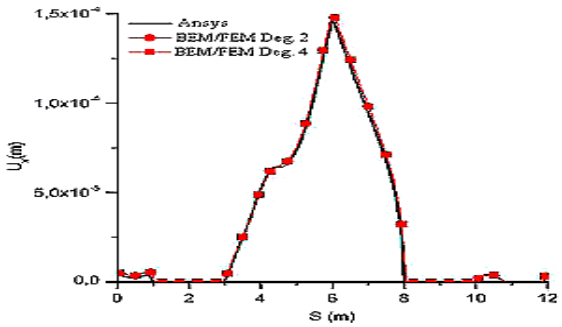

(a)

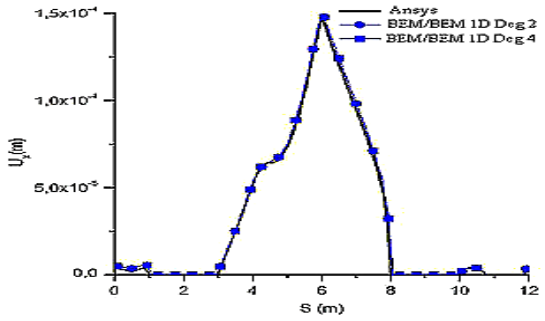

(b)

Fig.17
Displacements in *x* direction - Coupling Example.3.

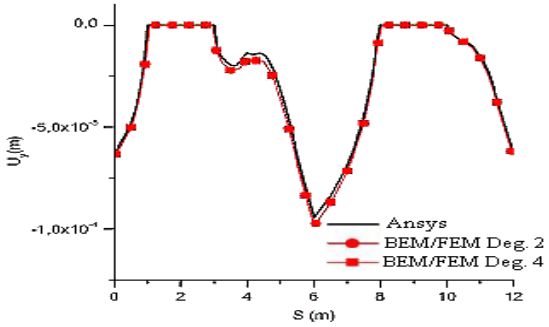

(a)

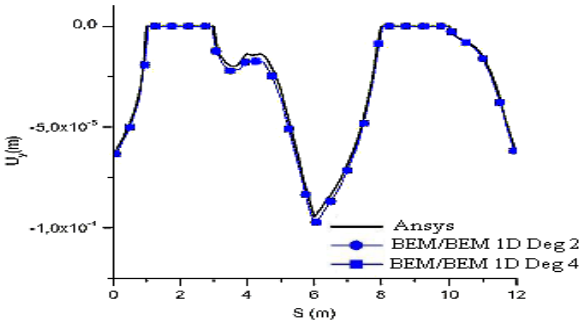

(b)

Fig.18
Displacements in *y* direction - Coupling Example.3.

As for support reactions, there are 2 sections in which the model is set, presenting stress concentration near the extremities.

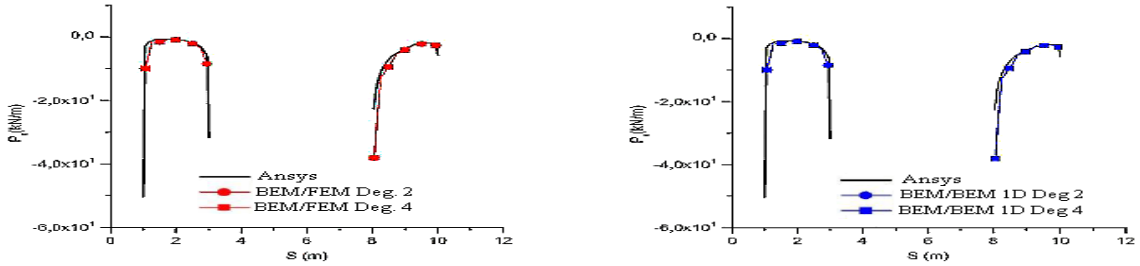

(a) (b)

Fig.19
Support reactions in *x* direction - Coupling Example.3.

4.3.2 Lower fiber

The results in lower fiber displacements were close, regardless of the method adopted:

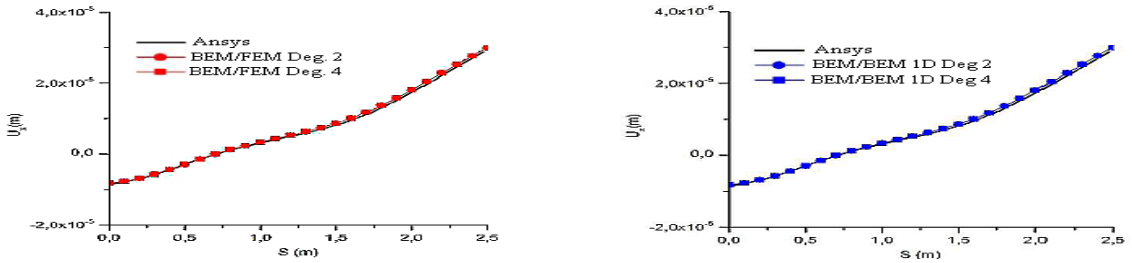

(a) (b)

Fig.20
Displacement *x* on the lower fiber - Coupling Example.3.

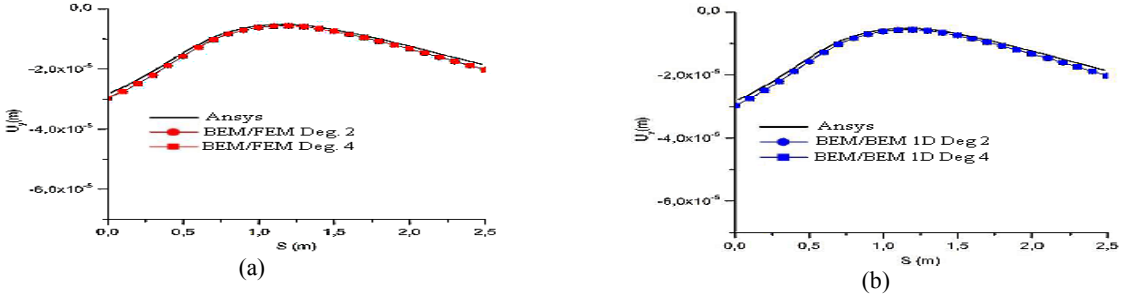

(a) (b)

Fig.21
Displacement *y* on the lower fiber – Coupling Example.3.

As for the adhesive force of results and normal force, BEM / FEM coupling had more unstable response in relation to the BEM / BEM 1D. It is found that near the stiffening tips there is a concentration of stress, the FEM finding it difficult to capture it:

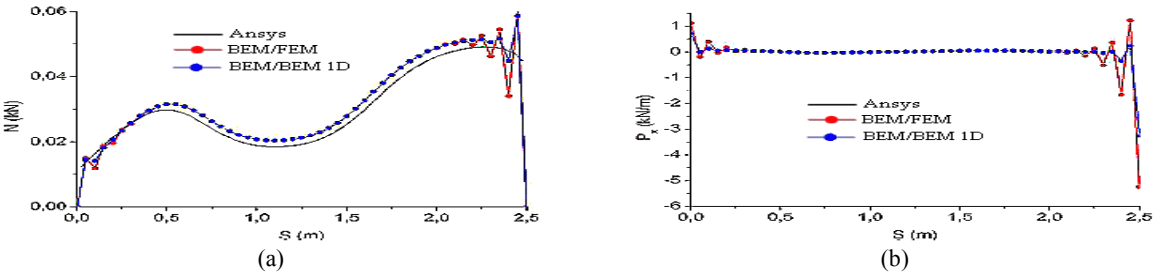

(a) (b)

Fig.22
Normal forces and adhesion forces on the lower fiber - Degree 2 - Coupling Example.3.

Using the fourth-degree approximation results convergence.

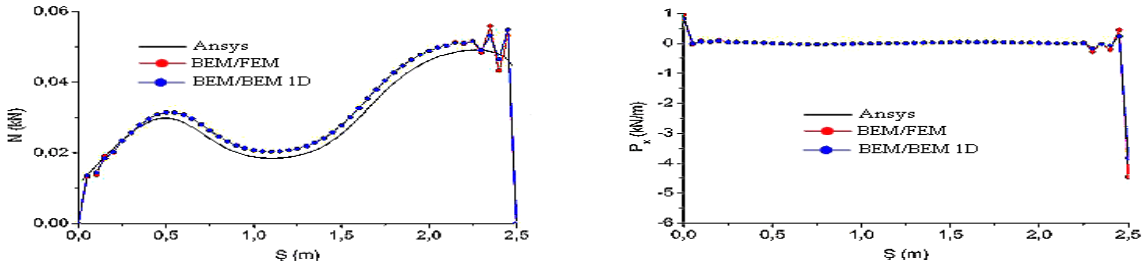

(a) (b)

Fig.23
Normal forces and adhesion forces on the lower fiber - Degree 4 - Coupling Example.3.

4.3.3 Superior fiber

Similar to the lower fiber, the results in upper fiber displacements were close.

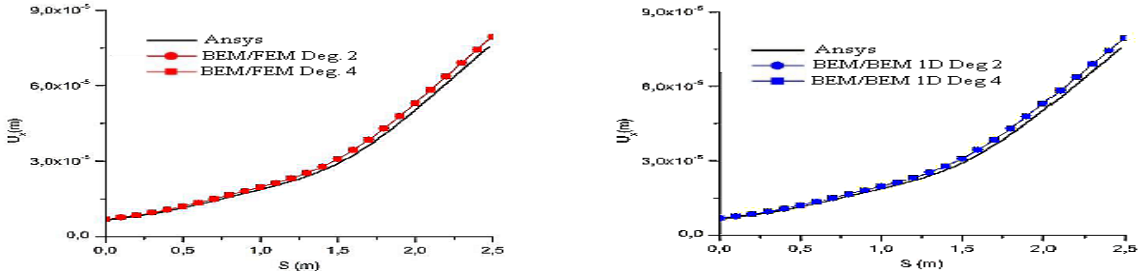

(a) (b)

Fig.24
Displacements in *x* on top fiber - Coupling Example.3.

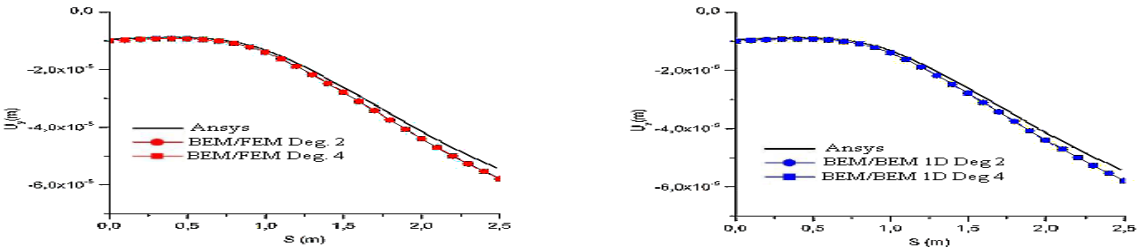

(a) (b)

Fig.25
Displacements in *y* on top fiber - Coupling Example.3.

In the case of normal force and adhesion force, the result of the BEM / FEM was also unstable near the tips.

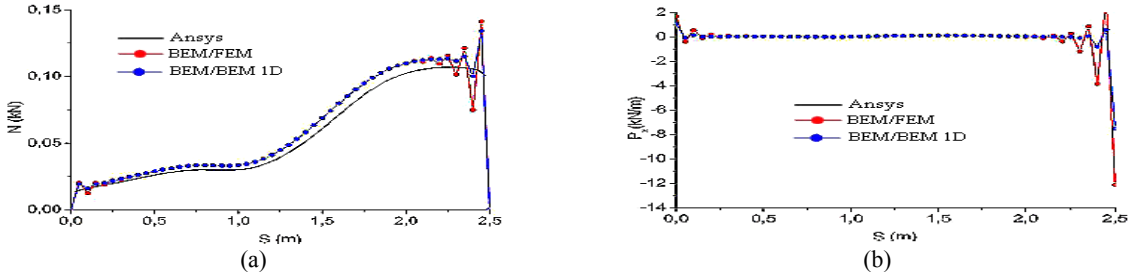

(a) (b)

Fig.26
Normal forces on top fiber - Grade 2 - Coupling Example.3.

Again, as the use of fourth degree approximation results convergence occurs.

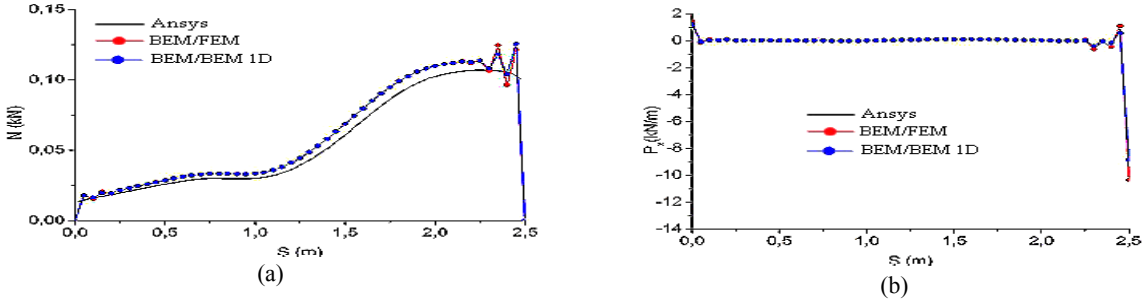

Fig.27
Normal forces on top fiber - Grade 4 - Coupling Example.3.

Even in the case of a problem with adverse contour and loading conditions, with the application of isotropic inclusion, the logic of the previous examples was maintained. Thus, BEM / FEM 1D presented greater stability for adhesion force and normal force results adopted regardless of the degree of approximation. In the case of BEM / FEM using quadratic approximation elements, perturbations were observed near the tips, requiring greater discretization of stiffeners to avoid them, or to increase the degree of approximation. However, with the use of fourth degree approximation the results of both methods were very close.

5 CONCLUSION

Having defined the mathematical bases in order to validate the formulation adopted for BEM 1D, two examples of truss bars with different loads were evaluated. Then the union and rotation of elements was evaluated, comparing with the academic computer program FTOOL. Good results were obtained in all, demonstrating the consistency of the formulation adopted.

An example of stiffened media with different discretization and degree of fiber approximation were evaluated. Maintaining the number of nodes, the use of quadratic, cubic and fourth degree approximations was evaluated. Clearly, it could be seen that stress concentration occurs at the fiber ends. For this reason, the change in discretization and the degree of approximation in these areas has the greatest effects, and increased discretization has the usual positive effect.

With the different examples performed, it can be concluded that the formulation adopted for coupling with BEM proved to be consistent, presenting convergence of results even with ANSYS. Good results were obtained even for the case of greater stiffness difference between stiffeners and medium. Modeling of stiffeners mainly affected in their own result in grip strength and normal strength, coupling with BEM 1D proving stable in all adopted situations. With the use of the fourth-degree approximation, BEM / FEM convergence with BEM / BEM 1D occurs, and in the second example there is a significant improvement of both methods. For this reason, it is therefore recommended to prioritize the use of fourth degree approaches and, in the case of lower degree approaches, to avoid coupling with the FEM.

Due to its complexity, example four of the coupling with the BEM had, among the analyzed, the highest computational cost. However even in this time the time was not high, being of the order of 40 seconds. There was no relevant difference between the methods.

REFERENCES

[1] Barzegar F., Maddipudi S., 1994, Generating reinforcement in FE modelling of concrete structures, *Journal of Structures Engineering* **20**(5): 1656-1662.

[2] Gomes H.M., Awruch A.M.S., 2001, Some aspects on three-dimensional numerical modelling of reinforced concrete structures using the finite element method, *Advances in Engineering Software* **32**(4): 257-277.

[3] LE V., Anh et Royer J., 1996, Boundary formulation for three-dimensional anisotropic crack problems, *Applied Mathematical Modelling* **20**(9): 662-674.

[4] Leonel E.D., 2006, *Boundary Element Method Applied to Analysis of Multi-Fractured Solids*, Sao Carlos, University of Sao Paulo.
[5] Leonel E.D., 2009, *Nonlinear Boundary Element Method Models for Fracture Problem Analysis and Application of Reliability and Optimization Models in Fatigue Structures*, São Carlos, Department of Structural Engineering.
[6] Oliveira Hugo Luiz et L., Edson D., 2013, Cohesive crack growth modelling based on an alternative nonlinear BEM formulation, *Engineering Fracture Mechanics* **111**: 86-97.
[7] Oliveira Hugo Luiz et L., Edson D., 2013, Dual BEM formulation applied to analysis of multiple crack propagation, *Key Engineering Materials* **2013**: 99-106.
[8] Nourine L., 2010, Boundary element method analysis of cracked anisotropic bodies, *The Journal of Strain Analysis for Engineering Design* **45**: 45-56.
[9] Sahli A., 2014, Failure analysis of anisotropic plates by the boundary element method, *Journal of Mechanics* **30**: 561-570.
[10] Sahli A., 2015, Effects of variation of material properties on the stress intensity factors of cracked anisotropic bodies, *Matériaux & Techniques* **103**: 109.
[11] Debbagui S., Sahli A., Sahli S., 2017, Optimisation and failure criteria for composite materials by the bound-ary element method, *Mechanics* **23**: 506-513.
[12] Kebdani S., Sahli A., Sahli S., 2018, Thermoelastic fracture parameters for anisotropic plates, *Journal of Solid Mechanics* **10**: 435-449.
[13] Sahli A., Fatiha Arab M., Sahli S., 2019, Composite parameters analysis with boundary element method, *Journal of Materials and Engineering Structures* **5**: 387-398.
[14] Kadri M., Sahli A., Sahli S., 2019, Fracture parameters for cracked cylindrical shells, *Journal of Solid Mechanics* **11**: 91-104.
[15] Sahli A., Sahli S., Mechanical and structural reliability-based algorithm optimization, *Journal of Materials and Engineering Structures* **6**: 215-232.
[16] Zienkiewicz O.C., Kelly D.W., Bettess P., 1977, The coupling of the finite element method and boundary solution procedures, *International Journal for Numerical Methods in Engineering* **11**(2): 355-375.
[17] Shaw R.P., Falby W., 1978, FEBIE—a combined finite element-boundary integral equation method, *Computers & Fluids* **6**(3): 153-160.
[18] Brebbia C.A., Georgiou P., 1979, Combination of boundary and finite elements in elastostatics, *Applied Mathematical Modelling* **3**(3): 212-220.
[19] Wearing J. L., Burstow M. C., 1994, Elasto-plasticanalysis using a coupled boundary element finite element technique, *Engineering Analysis with Boundary Elements* **14**(1): 39-49.
[20] Coda H.B., Venturini W.S., Aliabadi M. H., 1999, A general 3D BEM/FEM coupling applied to elastodynamic continua/frame structures interaction analysis, *International Journal for Numerical Methods in Engineering* **46**(5): 695-712.
[21] Coda H.B., Venturini W.S., 1999, On the coupling of 3D BEM and FEM frame model applied to elastodynamic analysis, *International Journal of Solids and Structures* **36**(31-32): 4789-4804.
[22] Elleithy W.M., Tanaka M., Guzik A., 2004, Interface relaxation FEM–BEM coupling method for elasto-plastic analysis, *Engineering Analysis with Boundary Elements* **28**(7): 849-857.
[23] Ganguly S., Layton J.B., Balakrishna C., 2000, Symmetric coupling of multi-zone curved Galerkin boundary elements with finite elements inelasticity, *International Journal for Numerical Methods in Engineering* **48**(5): 633-654.
[24] Bia R.A., Ostrowski Z., Kassab A.J., Yin Q., Sciubba E., 2002, Coupling BEM, FEM and analytic solutions in steady-state potential problems, *Engineering Analysis with Boundary Elements* **26**(7): 597-611.
[25] Coda H.B., 2001, Dynamic and static non-linear analysis of reinforced media: a BEM/FEM coupling approach, *Computers & Structures* **79**(31): 2751-2765.
[26] Leite L.G., Coda H.B., Venturini W.S., 2003, Two-dimensional solids reinforced by thin bars using the boundary element method, *Engineering Analysis with Boundary Elements* **27**(3): 193-201.
[27] Fernandes G.R., Venturini W. S., 2002, Non-linear boundary element analysis of plates applied to concreteslabs, *Engineering Analysis with Boundary Elements* **26**(2): 169-181.
[28] Brebbia C.A., Domınguez J., 1992, *Boundary Elements: An Introductory Course*, Computational Mechanics Publications, McGraw Hill Company, London.
[29] Cruz J. M. F., 2012, *Contribution to the Static and Dynamic Analysis of Frames by the Boundary Element Method*, Federal University of Paraíba.